1. Introduction

Apart from mass and chemical composition, the size distribution of fine particles represents a vital physical property with important implications for human health and environmental effects of ambient aerosols (Seinfeld and Pandis, 2006). Particle size relates directly to the aerodynamic properties which govern the penetration and deposition of particles in the airways and lungs (Davidson et al., 2005) as well as the scattering and absorption of light which affect the radiative properties and hence ambient visibility (Ahlquist and Charlson, 1967;Bohren and Huffman, 1983;Charlson et al., 1991;Schwartz, 1996;Seinfeld and Pandis, 2006). Hygroscopic growth in response to changes in ambient humidity can alter particle light scattering properties (Seinfeld and Pandis, 2006;Köhler, 1936) and activation of condensation nuclei particles into cloud droplets depend on atmospheric conditions, chemical composition, mixing state as well as the size and morphology of particles (Abbatt et al., 2005;Kerminen et al., 2012;Meng et al., 2014;Westervelt et al., 2013).

Studies into the size distribution of ambient particulate matter in Hong Kong have been largely based on size-segregated filter samples (Yao et al., 2007a;Zheng et al., 2008;Zhuang et al., 1999;Huang et al., 2014;Bian et al., 2014) and measurements by electrostatic classifier instruments (Cheung et al., 2015;Yao et al., 2007b) and were hence either limited in size resolution (offline filter samples) or chemical resolution (total particle count by classification). Most measurements in Hong Kong were conducted in suburban environments. Inorganic ammonium and sulfate were mainly found in fine mode particles in condensation and droplet mode size ranges, while nitrate had strong coarse mode contributions (Zhuang et al., 1999). Seasonal differences were evident in solvent-extractable organics and trace metals which were mainly found in $PM_{0.5}$ particles in the wet season and winter whereas in fall a shift to larger particles (0.5–2.5 μm fraction) in fall indicated a possibly stronger influence of aged particle components in the transition period of the Asian monsoon (Zheng et al., 2008). Size distributions acquired by a fast mobility particle sizer at the suburban HKUST supersite were investigated more recently to study the formation and accumulation of ultrafine particles under different air flow regimes. Particle number concentration enhancements during the day were attributed to secondary formation, while evening and nighttime peaks were thought to be related to transport of aged aerosols from upwind locations. Nucleation mode particle peaks were often observed in fall and related to regional pollution influence (Cheung et al., 2015). New particle formation events at the same site occurred as single and two-stage growth processes with organics and sulfuric acid contributing mainly to first stage growth in the daytime while nighttime second stage growth was attributed to ammonium nitrate and organics. Particle size growth into the diameter range of cloud condensation nuclei (CCN) was typically only achieved with the second growth stage (Man et al., 2015).

Investigations into particle size distributions in urban areas of Hong Kong are even scarcer. Yao et al. (Yao et al., 2007b) studied the properties and behavior of particles in vehicle plumes and reported a competing process between ambient background particles and fresh soot particles in the condensation of gaseous precursors and a dependency on temperature with bimodal volume size distributions observed at lower ambient temperatures and unimodal distributions in the lower accumulation size range at higher ambient temperatures.

The Aerodyne aerosol mass spectrometer (Canagaratna et al., 2007) is widely used to determine the chemical composition of major organic and inorganic components of non-refractory submicron particulate matter ($NR\text{-}PM_1$). In contrast to most traditional aerosol sizing instruments, the AMS is capable of resolving main chemical constituents

close to primary emission sources and a suburban location (coastal, HKUST supersite) which is largely a downwind receptor of varying amounts of local urban, regional and long-range transported pollutants (Li et al., 2015;Huang et al., 2014).

2. Methodology

2.1. Field campaigns

Sampling of ambient submicron non-refractory particulate matter (NR-PM_1) was carried out using an Aerodyne HR-ToF-AMS at the HKUST air quality supersite covering four seasons between May 2011 and February 2012 (spring: 2011-05, summer: 2011-09, fall: 2011-11&12, winter: 2012-02). The HKUST supersite is located on the campus of the Hong Kong University of Science and Technology (22°20'N, 114°16'E), on the east coast of Hong Kong in a suburban area with few primary emission sources in the immediate vicinity. Sampled air was drawn from the rooftop of a pump house building at an approximate height of 25m above ground level. For detailed descriptions of the experimental setup, operating conditions, data treatment, and overall species composition we refer the reader to previous publications (Lee et al., 2013;Li et al., 2015;Li et al., 2013). A further sampling campaign took place between spring 2013 (2013-03 to 2013-05) and summer 2013 (2013-05 to 2013-07) at an inner-city urban location in the densely populated and built-up Kowloon peninsula. Measurements were conducted next to the roadside air quality monitoring station (AQMS) operated by the Environmental Protection Department (EPD) of the HKSAR Government in the Mong Kok (MK) district on a pedestrian crossing at a major road junction. Sampled air was drawn from a height of 3m above ground level. A comprehensive analysis of trends in species concentration and composition identified in this urban campaign has been presented previously (Lee et al., 2015). In both campaigns, particles were sampled through a $PM_{2.5}$ cyclone at a flow rate of 16.67 L/min into a sampling port from which 0.08 L/min was drawn by the AMS and the remainder drawn by co-sampling instruments and an auxiliary pump. Sample air for the AMS passed through a 1m long diffusion dryer (BMI, San Francisco CA, USA) filled with silica gel to remove bulk gas- and particle-phase water. Additional data from various collocated instruments including meteorological data (wind, temperature, relative humidity, solar irradiation), volatile organic compounds (VOCs) and standard trace gases such as NO_x, SO_2, and O_3 were available.

AMS data were treated according to general AMS data treatment principles (DeCarlo et al., 2006;Jimenez et al., 2003) with standard software packages (SQUIRREL, PIKA). Analysis of the unit-mass resolution mass spectra yielded non-refractory submicron particle species concentrations of major inorganic constituents (SO4, NO3, NH4, Chl) and total organics at a base time resolution of 10 min. Positive Matrix Factorization (PMF) was used to deconvolute high-resolution organic mass spectra acquired at 10 min time resolution following recommended PMF guidelines for AMS data (Zhang et al., 2011) with the AMS PMF analysis toolkit (Ulbrich et al., 2009). At the urban Mong Kok site, six organic aerosol (OA) factors were identified encompassing three secondary organic aerosol (SOA) and three primary organic aerosol (POA) factors of which one was attributed to traffic emissions and two to cooking activities (Lee et al., 2015). Similarly, four factors were obtained from analysis of the urban HKUST site dataset with two SOA factors

be found in the Supplement (Text S1, Text S2). The sequence of main data treatment and analysis steps is shown in Fig. 1.

The transmission efficiency of the AMS aerodynamic lens is known to fall off below ~100nm and beyond ~550 nm of vacuum-aerodynamic diameter (Liu et al., 2007;Takegawa et al., 2009;Zhang et al., 2004;Bahreini et al., 2008;Williams et al., 2013;Knote et al., 2011) and may bias measured particle mass and mode diameters, particularly in the accumulation mode towards lower values if significant particle mass fractions fall in the size region of D_{va} > 550 nm. In the Aitken mode range, the effect of limited lens transmission is expected to be less substantial as particle volume (and hence particle mass) of Aitken mode particles are much smaller. We discuss the effects of lens transmission briefly in section 3.4. Delayed vaporization of particle components, e.g. under high mass loadings, can lead to small shifts towards larger mode diameters in AMS size distributions (Docherty et al., 2015) and enhanced tails in the size distributions (Cross et al., 2009), which may lead to larger fit residuals at the trailing edges. Generally, the discussion of size distributions in this work should be viewed in the context of the instrumental capabilities and previously mentioned limitations of aerosol mass spectrometry. Therefore, the resolved Aitken and accumulation modes in this work reflect the apparent Aitken and accumulation modes within AMS measurable particle mass size distributions.

378

Figure 4. Diurnal variations of mode diameter (MMD), integrated mode mass concentration and width of the Aitken mode (*lighter color*) and accumulation mode (*darker color*) from bimodal peak fits of the bin-median reconstructed size distributions at the suburban HKUST site and V-mode AMS species concentrations (line with shaded background) for organics, nitrate and sulfate (left to right) in (a) spring 2011, (b) summer 2011, (c) fall 2011 and (d) winter 2012; The right-most panel depicts the median diurnal variations of relevant gas-phase pollutants (O_3, CO, NO_x, SO_2) measured at the same site.

3.1.2. Suburban coastal NR-PM_1

The suburban HKUST site as a downwind receptor of urban and regional pollution was generally dominated by sulfate and oxygenated secondary organic aerosol (SOA) components and much lower fractions of primary organic constituents, which combined typically made up less than a quarter of total organics (Li et al., 2015). Trends in the species segregated particle size distributions are discussed analogously to section 3.1.1., with Fig. 4 illustrating the diurnal trends of the fitting parameters (MMD, integrated mode mass, geometric standard deviation) for organics, sulfate, and nitrate at the suburban HKUST site.

Organics

There were significant seasonal differences with larger fractions (Fig. 3b) and concentrations (Fig. 5c) of Aitken mode mass in total organic submicron particle mass in spring and summer compared to fall and winter, indicating greater influence of closer-ranged formation sources in the warmer season. Springtime integrated Aitken mode mass concentrations (~0.8 μg/m^3) were twice as high as those in winter (~0.4 μg/m^3). In the accumulation mode, highest particle mass loadings were observed in fall (5 μg/m^3) and lowest loadings in spring (3 μg/m^3) following the frequency pattern of continental air mass influence (Fig. S12 in the Supplement) in each season indicating continental transport of particulate mass or gas-phase precursors. Lowest mass concentrations in the Aitken mode typically occurred in the night hours (00:00 – 05:00) in a range of 0.3 – 0.5 μg/m^3 in spring, summer, and winter, while in fall mass loadings of 0.7 - 0.8 μg/m^3 were reached. Diurnal changes were least pronounced in winter with largely constant integrated Aitken mode particle concentrations. In the remaining seasons, varying degrees of daytime changes were apparent with a general increase around 06:00, likely owing to citybound commuter traffic from surrounding roads to the west of the sampling site at 1-2km of lateral distance. This also led to a modest increase in particle polydispersity with a discernible widening of the Aitken mode size distributions (*black solid line, lowest panels in* Fig. 3). Daily maxima in spring, summer and fall were reached in the early evening (~21:00) with marked differences in absolute mass concentrations depending on the respective season, from a summer time low of 0.8 μg/m^3 to a fall season high of 1.4 μg/m^3. Mass median diameters in the Aitken mode were smaller in the night hours and displayed subtle increments during the day in the range of 10-20 nm reaching their maximum typically in the late afternoon, except for the fall season when mass median diameters displayed very little variation with time of day.

Total particle mass in the accumulation mode in spring and summer reached minima during the night hours (2 μg/m^3) and maxima (3 μg/m^3) around noon, remaining stable in the daylight hours thereafter. MMDs increased notably from 440nm at night to 510nm during the day in spring, while in summer a morning rise by ~30nm from 530nm to 560nm was obvious between 06:00 and 10:00 and coincided with the morning rush hour and the associated early morning

peak of NO_x and an otherwise stable mode diameter of 530nm for the rest of the day. In fall, the increase in accumulation mode organic mass occurred much earlier, starting in the dark hours at 04:00, with a corresponding trend also evident for nitrate but absent for sulfate, indicating a common source of these organic and nitrate enriched particles. Nighttime MMDs for organics were generally larger (540nm) and decreased to a minimum of 510nm in the early afternoon accompanied by a slight widening of the distribution. In winter, mass concentrations decreased appreciably in the early morning hours and started to increase only beyond 10:00. In the colder seasons (fall, winter), a similar concentration pattern was also observed for gas-phase SO_2 which is considered as a largely regional pollutant with few distinct local sources (Yuan et al., 2013), indicating that changes in boundary layer and mixing with regional background were likely the more dominant processes in winter.

Sulfate

Aitken mode sulfate mass concentrations peaked in the afternoon from spring throughout fall with maximum concentrations reached progressively later in the afternoon (14:00 in spring; 16:00 in fall). Nominal concentrations were highest in spring and summer (0.5-0.6 $\mu g/m^3$), slightly lower in fall (0.4 $\mu g/m^3$) and reached the lowest levels in winter (0.1 $\mu g/m^3$). In addition to the afternoon peak, a conspicuous early morning peak of similar magnitude was evident in spring between 02:00 and 06:00. A greater proportion of southerly winds was evident in said time period compared to the overall seasonal wind frequency distribution (Fig. S13a in the Supplement) and may indicate transport of sulfate from marine sources in the southern parts of Hong Kong. Diurnal variations in MMDs and GSDs were generally small and without obvious regular trends. Nominal mass median diameters were significantly lower in winter (~170nm) compared to spring and fall (~190nm) and summer (~210nm).

Trends in accumulation mode particle mass were more pronounced. In spring, a shallow concentration valley during the late evening and night hours (20:00 to 03:00) with minimum concentrations of 5 $\mu g/m^3$ was apparent, while daytime concentrations stayed largely invariant at 6 $\mu g/m^3$. The MMDs followed a similar variation with a minimum mode diameter around 550nm in the early hours of the day and slightly larger daytime MMDs around 570nm. Nominal concentrations were larger in summer with a nighttime valley concentration of 7 $\mu g/m^3$ and a well-pronounced broad day peak with a maximum of 9.5 $\mu g/m^3$ in the early afternoon (14:00-15:00). A prior additional morning peak occurred between 04:00 and 10:00 with particle mass concentrations reaching 8.5 $\mu g/m^3$ related to a consistent north-easterly morning wind pattern (Fig. S13b in the Supplement) and likely associated with transport from north-easterly coastal regions or nighttime fisheries related maritime traffic. The diurnal trend in mass median diameter was similar to that in spring with a night minimum of 570nm and day maximum of 590nm.

In fall, accumulation mode characteristics showed no significant diurnal variability, with a largely stable integrated particle mass of 6 $\mu g/m^3$ and only subtle MMD changes (585nm at night; 575nm during the day). In winter, two concentration dips with reductions by ~0.5 $\mu g/m^3$ between 06:00 and 10:00 and between 18:00 and 22:00 were evident, while MMDs increased during the day between 10:00 and 15:00 from 520nm, peaking at a size of 540nm.

Nitrate

Nitrate particle mass in the Aitken mode was generally small from spring throughout fall amounting to 0.01 - 0.06

μg/m^3. Winter time concentrations were larger in a range of 0.06 - 0.08 μg/m^3 during the day and 0.10 - 0.12 μg/m^3 in the late evening hours. The latter evening peak centered around 21:00 was evident in most seasons (except spring) and accounted for 12-23% (0.1-0.25 μg/m^3) of total daily Aitken mode nitrate mass burden. Similar to the urban roadside location, these nighttime nitrate peaks coincided with the peak period of organic cooking aerosol concentrations (Fig. S14 in the Supplement), which were however significantly smaller at the suburban measurement site and mainly attributed to the operation of an on-campus student canteen (Li et al., 2015). Trends in mass median diameters varied between seasons with no discernible trend in winter, a subtle decreasing trend with time of day in spring and broad daytime diameter increases in summer and fall. Solar irradiation in these two seasons was comparatively high (Fig. S10b-c in the Supplement) indicating that photochemical nitrate production in the Aitken mode may have led to this observed growth in particle size.

Integrated particle mass concentrations in the accumulation mode only exhibited subtle variations from spring throughout fall, with essentially constant diurnal concentrations in spring, a subtle daytime peak in summer which accounted for ~ 15% of total daily accumulation mode nitrate (corresponding to 0.7 μg/m^3) and a conspicuous morning peak between 04:00 and 10:00 in fall accounting for ~ 5% of total daily accumulation mode nitrate (corresponding to 0.5 μg/m^3). Clearer seasonal differences were evident in the trends of MMDs. In spring, MMDs decreased appreciably over the late evening hours (21:00-0:00) with a concurrent widening of the size distribution (increase in GSD). In summer, accumulation mode diameters decreased during the day by ~40nm with a similar trend in accumulation mode organics. Winter time MMDs exhibited a more complex pattern with larger mode diameters in the early hours (04:00 – 10:00) and during the noon-time, and a late-afternoon dip leading to larger spread of intra-day mode diameters ranging from 510nm to 570nm.

In comparison to the urban roadside measurements, diurnal particle size characteristics and mass concentrations in the Aitken and accumulation mode were much more variable for all investigated species at the suburban HKUST site, indicating that longer time scale processes and irregular events (transport patterns, local meteorology) were probably more important in governing particle size distribution characteristics than diurnal processes.

3.2. Day-to-day size distributions and seasonal averages

To evaluate the evolution of particle size distributions within seasons, average species-specific size distributions were generated by averaging raw distributions over 24h periods (between 0:00 and 23:59). There was clear long-term variability in both resolved Aitken and accumulation mode MMDs and integrated submode particle mass concentrations for all species (Fig. S15-16 in the Supplement) and overall seasonal differences which have been briefly addressed in the discussion of the diurnal size distribution variations between seasons. Figure 5 depicts the overall average values for all daily fitted MMDs and integrated particle mass concentrations in both the Aitken and accumulation mode at the suburban HKUST and urban MK sites.

3.2.1. Seasonal trends

For the MK roadside station, particle mode diameters were generally larger in spring than in summer for all three investigated species, but with clear differences in the magnitude of changes among individual species. In the Aitken mode, organics and sulfate displayed a moderate decrease in mode diameter from spring to summer by 7-8% each, while nitrate saw a more significant decrease by 25% from spring to summer. In contrast, accumulation mode MMDs for organics exhibited only a subtle decrease by 5% and more substantial decreases for sulfate and nitrate by 20-22% each. Total Aitken mode particle mass decreases varied strongly: -15% for organics, -36% for sulfate and -67% for nitrate. In the accumulation mode, organics and sulfate exhibited similar relative decreases by 40-46%, while nitrate particle mass reduced drastically by 85%.

At the suburban HKUST site, Aitken mode MMDs of nitrate and organics decreased with the progression of seasons from spring to winter with highest mode diameters observed in spring and summer and appreciable decreases in winter by -9% for nitrate and -25% for organics compared to the warmer seasons. Sulfate displayed a similar winter time decrease in MMD (-15%) and an increase of similar magnitude in the summer season (+13%) compared to spring and fall. Variations in sulfate and organic accumulation mode diameters were minor between spring and fall, while wintertime MMDs were 7-12% lower. Nitrate exhibited an overall higher variability in mass median diameters in the accumulation mode in spring (larger standard deviation) and with on average 10% lower MMDs compared to other seasons. In line with the reduction in Aitken mode MMDs in winter, the integrated Aitken mode particle mass decreased as well, by -16% for organics and almost -75% for sulfate, whereas nitrate contributions remained largely stable throughout the seasons. Organic accumulation mode particle mass was significantly higher in the fall and winter season by factors of 1.6 – 2. Diurnal variations in the degree of oxygenation were least pronounced in these seasons (Li et al., 2015) suggesting that influence of transport in autumn and winter likely dominated over local formation, thus exerting greater effects on particle mass in the larger size mode. Particulate nitrate concentrations were generally low in the accumulation mode from spring through fall, but increased sharply in winter by factors of 3 – 4. Sulfate accumulation mode mass concentrations remained more stable but saw significant summer time enhancements by ~30% likely due to photochemical activity which also led to high concentrations of Ox and a higher degree of oxygenation of organic aerosol among the four seasons (Li et al., 2015).

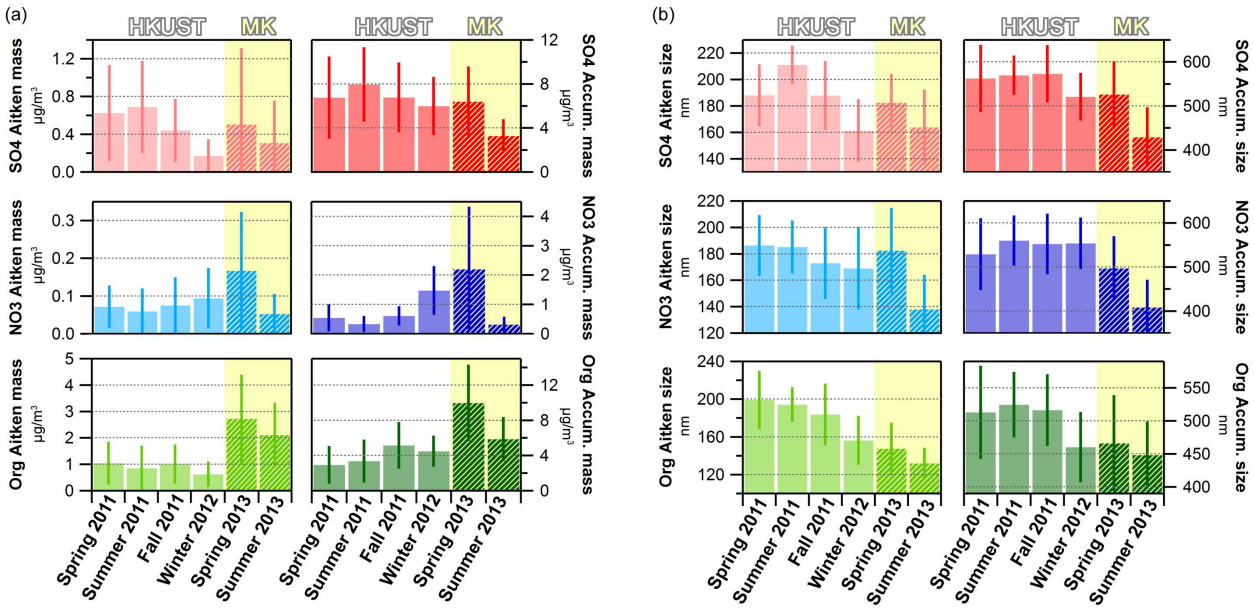

Figure 5. Average and standard deviation of daily fit values of Aitken and accumulation mode particle mass and mass median diameters at the suburban HKUST site (*solid bars*) and urban MK site (*hashed bars*). The integrated particle mass is depicted in (a) for the Aitken mode (*left panels*) was well as the accumulation mode (*right panels*) for sulfate, nitrate, and organics respectively. The mass median diameter is depicted in (b) for the Aitken mode (*left panels*) as well as the accumulation mode (*right panels*) for sulfate, nitrate and organics respectively.

Large particles contribute more to particle volume and hence particle mass. Correspondingly, the total submicron concentration of a given species is typically governed by changes in the accumulation mode particle mass and accordingly observed correlation values between integrated accumulation mode particle mass and individual NR-PM_1 species mass concentrations were generally high (R_{pr}>0.90) at both measurement sites (Fig. S17 in the Supplement). This applied to both measurement sites regardless of the season. Aitken mode trends were less akin. At the urban roadside station, neither sulfate nor nitrate particle mass in the Aitken mode notably correlated with the respective total submicron species mass concentration in spring (all R_{pr}≤0.20), whereas in summer correlations were more significant with R_{pr}=0.51 for sulfate and R_{pr}=0.80 for nitrate. This signifies that periods of greater species mass concentrations were more likely to be caused by increases in both Aitken and accumulation mode particle mass indicating that particle formation and growth affecting smaller particles was more likely to occur in the warmer season. For organics, Aitken mode particle mass and submicron species mass correlated only weakly (R_{pr} = 0.26 in spring and R_{pr} = 0.38 in summer), i.e. each organic particle submode was governed by largely different dominant sources or formation processes in both seasons at the roadside.

At the suburban background site, Aitken mode particle mass for sulfate showed little correlation with total submicron sulfate concentration (R_{pr}≤0.10) apart from the spring season (R_{pr}=0.36) where more frequent wet and foggy conditions may have facilitated sulfate formation in both size modes. For organics and nitrate significantly larger correlation coefficients of submode particle mass to total species concentration ($0.5 \leq R_{pr} \leq 0.7$) were observed in most seasons (spring, summer, winter) indicating significant influence of local or regional formation processes on

organic and nitrate Aitken mode particulate mass at the suburban receptor location. In the fall season, much weaker correlations ($0.2 \leq R_{pr} \leq 0.4$) were likely caused by the dominance of continental air mass influence (Fig. S12c in the Supplement) and greater influence of aged accumulation mode particles on total submicron nitrate mass concentrations.

3.2.2. Inferred changes in mixing state

Shifts in mixing state of ambient particles can be inferred from the inter-species analysis of mass median diameters. Close nominal agreement (i.e. diameter ratios close to 1) infer that different species were distributed similarly across the particle size range which thus most likely represents a largely internally mixed particle population, while the spread of data (correlation coefficient) indicates the temporal homogeneity or divergence of resolved mode diameters. A hypothetically perfectly internally mixed particle population over the whole sampling period would, therefore, yield MMD ratios and Pearson's R values of 1 between species, while larger or smaller values are indicative of a greater frequency of heterogeneous (i.e. more externally mixed) particle populations (Fig. 6).

At the urban Mong Kok site, changes in accumulation mode mass median diameters for nitrate and sulfate followed similar trends (R_{pr} = 0.88-0.89) and with diameter ratios close to 1 (0.94–0.95) Similarly, fitted accumulation mode diameters of organic constituents predominantly followed that of sulfate in spring nominally (diameter ratio 0.88) and temporally (R_{pr} = 0.80). The nominal agreement of organic and sulfate accumulation mode diameters persisted (diameter ratio 1.03) overall in summer, however, there was significantly more temporal divergence (R_{pr} = 0.65) indicating a greater frequency of time periods with external mixing of particle populations comprising different fractions of organic constituents.

External mixing is more prevalent for freshly formed smaller particles which have typically undergone less condensational growth, coagulation or aqueous-phase reactions. Indeed, the correlation coefficients of both nitrate and organic Aitken mode MMDs with respect to sulfate were notably lower (0.50 and 0.62) indicating frequent periods of particle populations with different species prevailing in different size regions within the Aitken mode.

Sulfate and nitrate were still more likely to occur internally mixed in the Aitken mode in spring with similar diameters (nitrate to sulfate MMD ratio = 1.00), while organic Aitken mode MMDs were consistently lower, indicating greater fractions of organic dominated particles towards the lower end and more inorganic dominated particles towards the upper end of the fitted Aitken mode.

In summer, both nitrate and organic MMDs tended to be lower than those of sulfate (diameter ratios of 0.79 – 0.83) but similar to each other, thus implying a shift to externally mixed populations of more nitrate and organic enhanced and internally mixed smaller Aitken mode particles and sulfate dominated larger Aitken mode particles.

At the suburban HKUST site, accumulation mode MMDs of both nitrate and organics were generally quite similar to those of sulfate with diameter ratios of 0.88 – 1.06. Compared to the urban site, correlation coefficients of nitrate and sulfate were consistently lower (0.54 – 0.67) indicating a much greater frequency of time periods where sulfate and nitrate dominated particles in the accumulation exhibited significantly different particle size distributions.

In winter, organic MMDs were consistently lower than those of sulfate and nitrate indicating a greater proportion of externally mixed particle populations with organics enriched particles in the lower accumulation size range and inorganic dominated particles in the larger accumulation size range. The least variability in particle size was observed in the summer season where MMDs in both Aitken and accumulation mode displayed variations in relatively narrow ranges between 200-250nm and 500-700nm, whereas in the remaining seasons time periods with particle populations of lower MMD were more frequent, extending to MMDs as low as 100nm in the Aitken mode and 300nm in the accumulation mode.

In the Aitken mode, mass median diameters overall were quite similar across species, with diameter ratios of organic and nitrate distributions to those of sulfate in the range of 0.87 – 1.06, indicating that they generally covered a similar size range. The temporal agreement was highly variable with correlation coefficients (R_{pr}) spanning from 0.21 to 0.75 indicating that Aitken mode particle populations at the suburban site were generally more diverse and likely influenced by a greater range of particle formation and growth mechanisms compared to the urban Mong Kok site.

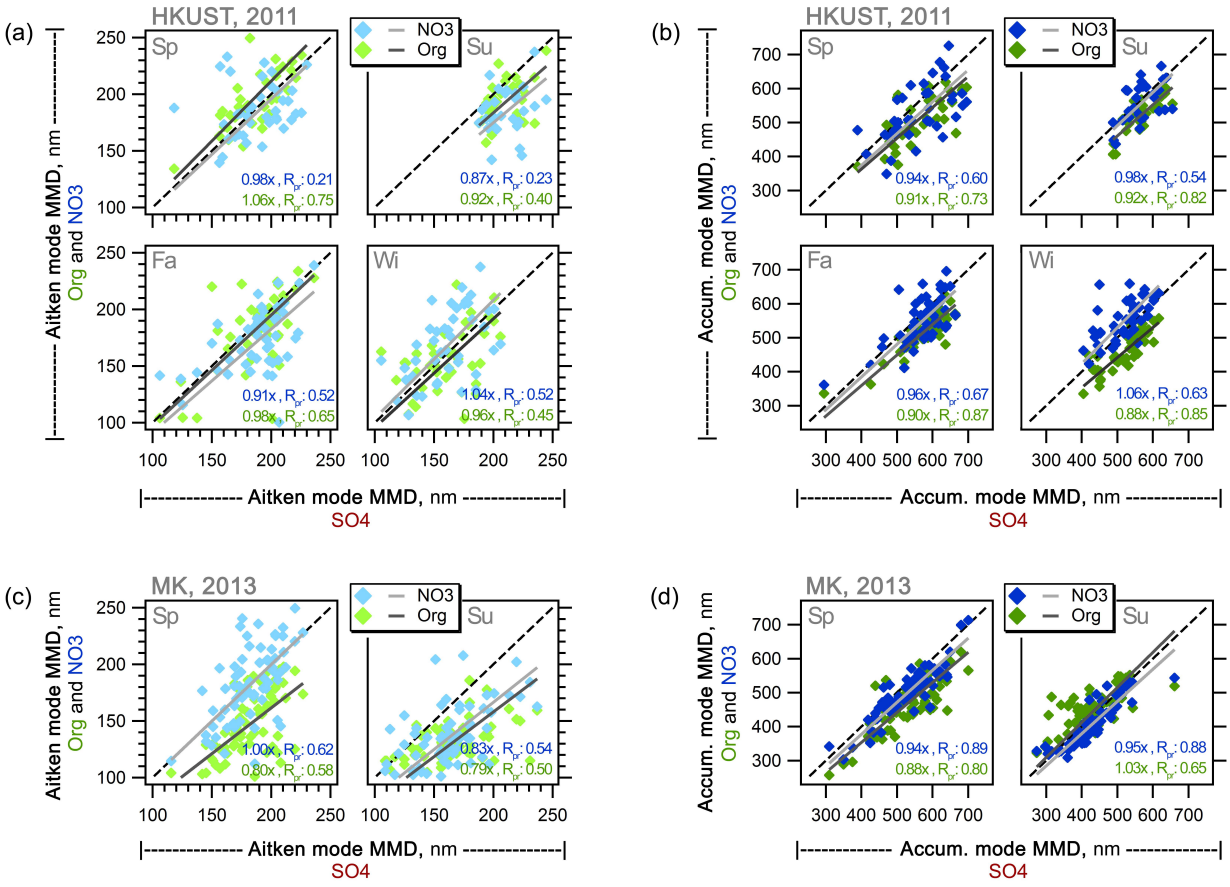

Figure 6. Scatter plots of fitted mass median diameters of organics and nitrate vs. sulfate for (a) the Aitken mode and (b) the accumulation mode at the HKUST suburban site, and (c) the Aitken mode and (d) the accumulation mode at the urban Mong Kok site

3.3. Comparison to previous studies

Particle size distribution studies in Hong Kong are generally scarce and have focused on either size segregated filter samples (MOUDI) for general ambient measurements or electrostatic classification in particle formation and particle growth studies (Guo et al., 2012;Cheung et al., 2015) . The latter studies focus on specific and narrow time periods and lack general discussions on ambient particle size distributions.

Two ambient studies were undertaken at the suburban coastal HKUST site using size-segregated samples from a ten-stage MOUDI sampler and offline chromatographic analysis. Inorganic constituents (NH4, NO3, SO4) in fine particles (i.e. D_p<1.8 µm) were shown to follow bimodal distributions with mode diameters in the range of 0.14-0.21 µm and 0.46-0.58 µm in samples collected in the winter season, while the main mode was observed in the coarse region (4-6 µm) for all three species (Zhuang et al., 1999). A subsequent year-long observational study also reported bimodal fine particle distributions with mode diameters of 0.1-0.3 µm and 0.7–0.9 µm and 1-2 additional modes in the coarse region (Bian et al., 2014), however, the main mode in the size distributions of sulfate, ammonium, potassium and oxalate was observed in the droplet mode (0.7 – 0.9 µm) in this study. Vehicle exhaust plumes sampled on-road from a Mobile Real-time Air Monitoring Platform (MAP) across Hong Kong's road network exhibited three distinct particle volume size distributions: a unimodal distribution with an accumulation mode at 0.2 µm and two bimodal distributions with a minor mode at 0.2 µm and the dominant mode at 0.5 or 0.7 µm (Yao et al., 2007b).

The bimodality in the fine particle range across these studies is consistent with the AMS-based results in this work. Nominally, the accumulation mode diameters from filter based studies and the chase studies are larger than those from AMS measurements where maximum mode diameters occurred at D_{va} ~ 700nm, corresponding to D_a ~ 470 (assuming D_{va} ~ D_a * density; particle density ~ 1.5 g/cm^3). Direct comparability is however limited due to fundamental differences in sizing techniques (MOUDI: atmospheric pressure; AMS: near-vacuum), sampling times (MOUDI: 24h samples, scattered time line; AMS: minute raw resolution averaged to hourly or daily, continuous time line), measurement uncertainties (MOUDI: sampling artifacts such as vapor adsorption and desorption; AMS: inlet lens transmission) and aerosol pretreatment (none for MOUDI with potential impacts on particle size in high humidity (>80%) conditions (Fang et al., 1991); AMS: removal of water prior to introduction to instrument).

3.4. Influence of AMS lens transmission

The quantitative measurement of particle components in the AMS is dependent on three major factors which may lead to particle loss prior to detection (Huffman et al., 2005). Irregularly shaped particles deviating from the flight path in the vacuum chamber may miss the vaporizer. Particles bouncing off the vaporizer surface will not be vaporized and hence may not be detected. Lastly, the aerodynamic lens which is part of the instrument's inlet system does not transmit particles uniformly across all particle diameters. Small particles are lost due to insufficient focusing or diffusion and large particle impact the lens apertures (Liu et al., 2007;Williams et al., 2013). Being a function of particle size, the latter factor affects both total AMS quantifiable particle mass (NR-PM_1) and measured mass size distributions. Transmission curves determined for the standard lens, which is fitted in most AMS instruments, can

vary but typically show efficient (i.e. close to 100%) transmission in the range of 100-550nm (Knote et al., 2011) falling of significantly at either edge.

We examined the potential impact of lens transmission on the AMS mass size distributions on a number of 24h size distributions from the fall season HKUST dataset covering both efficient and reduced lens transmission size regimes (accumulation mode diameters between 400 and 600nm). Panels a-c in Fig. S18 in the Supplement depict original and lens-transmission corrected 24h mass size distributions for organic, nitrate and sulfate, assuming the transmission function (subpanel d) reported by Liu et al., 2007. Impacts were generally larger in the accumulation mode range with evident shifts to larger mode diameters and larger mode mass concentrations observed in all size distributions. In the small diameter range, enhanced shoulders can occur which may however be artifacts due to the larger uncertainties (low signal to noise ratio at small particle mass), i.e. greater noisiness at the leading end of AMS size distributions. For a quantitative comparison, bimodal fitting parameters from the corrected distributions were plotted against those from, the original distributions in Fig. S18 in the Supplement (subpanels e-g refer to the Aitken mode and subpanels h-j to the accumulation mode). Leading edge shoulders in the corrected size distributions were not considered in the fitting. Changes in the Aitken mode mass median diameters were minor (on average ~3%), while the integrated mode particle mass increased moderately (~48%). In the accumulation mode, mass median diameters increased by ~28% and integrated mode particle mass doubled. The distribution widths (geometric standard deviations) exhibited little change in both modes (increases of 2-3%).

Fitting results will therefore vary depending on whether AMS size distribution and concentration data are corrected for lens transmission. While explicit lens transmission corrections can improve the accuracy of quantification of AMS species concentration and size distribution measurements, few ambient studies explicitly use lens transmission corrections based on individual experimental determinations or literature values e.g. (Quinn et al., 2006;Cross et al., 2007). Lens transmission curves can vary between instruments (Fast et al., 2009) and are inherently difficult to determine accurately experimentally. As discussed previously, scaling of size distributions by lens transmission curves may introduce artifacts in noisier size distributions (e.g. low end of the Aitken mode, low concentration periods, short term size distribution averages). Trailing edges from slow vaporization (e.g. under high particle mass loadings) may be exacerbated and inflate mass concentrations at the upper size cut range of the AMS. The majority of ambient studies employs a combined correction factor (collection efficiency, CE) considered to be the joint product of the previously mentioned transmission efficiencies related to particle bounce, beam broadening and lens transmission (Middlebrook et al., 2012) derived from aerosol composition and by comparison to collocated speciation or particle sizing instruments. As the AMS lens transmission curve could not be determined in this study and to avoid additional uncertainties from the application of non-instrument specific lens transmission values, we followed the CE correction method in the analysis of the size distribution data in this study. The reported values of resolved mode diameters and integrated mode should therefore be regarded as lower bound estimates in the context of the instrumental limitations affecting ambient AMS measurements.

4. Conclusion

A detailed analysis of AMS mass-based particle size distributions of sulfate, nitrate, and organics in submicron particulate matter measured at two contrasting locations in Hong Kong during two field campaigns has been undertaken. Deconvolution of size distributions into Aitken and accumulation submodes was accomplished by log-normal peak fitting and trends in particle size (mass median diameters), dispersity (geometric standard deviation) and overall particle mass (integrated mode area) were discussed on a diurnal time scale and on a daily basis to evaluate longer-term changes in size distribution characteristics. At the urban roadside location, clear diurnal influences of primary particle and gas-phase species were evident affecting both inorganic and organic component size distributions. Traffic and cooking contributed an estimated 0.3 – 0.9 μg/m^3 and 0.5 – 1.8 μg/m^3 of organic component particle mass in the Aitken mode, and 1.6 - 1.8 μg/m^3 and 1.0 – 2.7 μg/m^3 respectively in the accumulation mode with concentrations level varying with seasons. Notable changes in Aitken mode mass median diameters of organics were limited to the morning rush hour. Daytime particle concentration maxima of sulfate and nitrate in summer indicated substantial influence of photochemical processes, which also led to increments in mass median diameters in the accumulation mode thus inferring associated particle growth. Nocturnal nitrate formation was apparent in the accumulation mode in spring concurring with the nighttime peak of ozone at the roadside, while in the Aitken mode nitrate particle concentrations were significantly elevated during the dinner hours. Organics-related size distributions were mostly governed by intra-day changes at the urban site with very similar trends across different size distribution sets (i.e. concentration regimes), while disparities in diurnal variations among different size distribution sets were evident for nitrate and sulfate, particularly affecting the average sets, indicating stronger influence of irregular external factors which were not associated with diurnal time scale processes.

Suburban particle size distributions exhibited variable diurnal characteristics, suggesting that irregular processes such as transport and seasonal meteorological conditions were the more dominant processes influencing particle size characteristics. Aitken mode particle mass of organics was significantly larger in spring and summer indicating greater influence of more local formation sources in the warm season. In the accumulation mode, organic particle mass concentrations were highest in fall and lowest in spring, following the frequency pattern of continental air mass influence. For sulfate, Aitken mode mass concentrations mass concentrations peaked in the afternoon from spring throughout fall with highest nominal concentrations in spring and summer and lowest levels in winter, while accumulation mode particle mass was highest in summer and fall and lowest in winter, similar to the trend observed among organic constituents.

Nitrate particle mass in the Aitken mode was generally small in most seasons (0.01 - 0.06 μg/m^3), except winter where daytime concentrations reached ~0.1 μg/m^3. In both modes, changes in mass median diameters varied temporally and in magnitude with seasons, indicating a stronger influence of specific meteorological conditions on the properties of nitrate-containing particles at the suburban site. At the urban site, periods of greater inorganic species mass concentrations were more likely to be caused by increases in both Aitken and accumulation mode particle mass in summer, indicating that particle formation and growth affecting smaller particles was more likely to occur in the warmer season. At the suburban receptor location, significant correlation of submode particle mass to total species concentration ($0.5 \leq R_{pr} \leq 0.7$) was observed for organics and nitrate in most seasons (spring, summer, winter)

suggesting notable influence of local or regional formation processes on organic and nitrate Aitken mode particulate mass. Variations in particle mixing state were examined by evaluation of inter-species mass median diameter trends at both measurement sites. In the accumulation mode at the urban site, internal mixing appeared to be prevalent in spring, while greater frequency of time periods with external mixing of particle populations comprising different fractions of organic constituents was observed in summer. External mixing was predominant in the Aitken mode at the urban location in both seasons. At the suburban site, sulfate and nitrate in the accumulation mode more frequently exhibited differing particle size distributions in all seasons signifying a greater extent of external mixing. In winter, external mixing of more organics enriched particles in the lower accumulation size range was evident.

Data availability

The data is available upon request. To obtain the data, please contact Chak K. Chan (chak.k.chan@cityu.edu.hk).

Competing interests

The authors declare that they have no conflict of interest.

Acknowledgements

This work was supported by the Environmental Conservation Fund of Hong Kong (project number ECWW09EG04). Chak K. Chan gratefully acknowledges the startup fund of the City University of Hong Kong.

References

Abbatt, J. P. D., Broekhuizen, K., and Kumal, P. P.: Cloud condensation nucleus activity of internally mixed ammonium sulfate/organic acid aerosol particles, Atmos. Environ., 39, 4767-4778, https://doi.org/10.1016/j.atmosenv.2005.04.029, 2005.

Ahlquist, N. C., and Charlson, R. J.: A New Instrument for Evaluating the Visual Quality of Air, J. Air Pollut. Control Assoc, 17, 467-469, https://doi.org/10.1080/00022470.1967.10469006, 1967.

Aiken, A. C., Salcedo, D., Cubison, M. J., Huffman, J. A., DeCarlo, P. F., Ulbrich, I. M., Docherty, K. S., Sueper, D., Kimmel, J. R., Worsnop, D. R., Trimborn, A., Northway, M., Stone, E. A., Schauer, J. J., Volkamer, R. M., Fortner, E., de Foy, B., Wang, J., Laskin, A., Shutthanandan, V., Zheng, J., Zhang, R., Gaffney, J., Marley, N. A., Paredes-Miranda, G., Arnott, W. P., Molina, L. T., Sosa, G., and Jimenez, J. L.: Mexico City aerosol analysis during MILAGRO using high resolution aerosol mass spectrometry at the urban supersite (T0) - Part 1: Fine particle composition and organic source apportionment, Atmos. Chem. Phys., 9, 6633-6653, https://doi.org/10.5194/acp-9-6633-2009, 2009.

718 Bahreini, R., Dunlea, E. J., Matthew, B. M., Simons, C., Docherty, K. S., DeCarlo, P. F., Jimenez, J. L., Brock, C.
719 A., and Middlebrook, A. M.: Design and operation of a pressure-controlled inlet for airborne sampling with
720 an aerodynamic aerosol lens, Aerosol Sci. Technol., 42, 465-471,
721 https://doi.org/10.1080/02786820802178514, 2008.
722 Bian, Q., Huang, X. H. H., and Yu, J. Z.: One-year observations of size distribution characteristics of major aerosol
723 constituents at a coastal receptor site in Hong Kong – Part 1: Inorganic ions and oxalate, Atmos.
724 Chem. Phys., 14, 9013-9027, https://doi.org/10.5194/acp-14-9013-2014, 2014.
725 Bohren, C. F., and Huffman, D. R.: Absorption and scattering of light by small particles, in: Absorption and
726 Scattering of Light by Small Particles, Wiley-VCH Verlag GmbH, 1-11, 1983.
727 Canagaratna, M. R., Jayne, J. T., Jimenez, J. L., Allan, J. D., Alfarra, M. R., Zhang, Q., Onasch, T. B., Drewnick, F.,
728 Coe, H., Middlebrook, A., Delia, A., Williams, L. R., Trimborn, A. M., Northway, M. J., DeCarlo, P. F.,
729 Kolb, C. E., Davidovits, P., and Worsnop, D. R.: Chemical and microphysical characterization of ambient
730 aerosols with the aerodyne aerosol mass spectrometer, Mass Spectrom. Rev., 26, 185-222,
731 https://doi.org/10.1002/mas.20115, 2007.
732 Charlson, R. J., Langner, J., Rodhe, H., Leovy, C. B., and Warren, S. G.: Perturbation of the Northern-Hemisphere
733 Radiative Balance by Backscattering from Anthropogenic Sulfate Aerosols, Tellus A, 43, 152-163,
734 https://doi.org/DOI 10.1034/j.1600-0870.1991.00013.x, 1991.
735 Cheung, K., Ling, Z. H., Wang, D. W., Wang, Y., Guo, H., Lee, B., Li, Y. J., and Chan, C. K.: Characterization and
736 source identification of sub-micron particles at the HKUST Supersite in Hong Kong, Sci. Total Environ.,
737 527-528, 287-296, https://doi.org/10.1016/j.scitotenv.2015.04.087, 2015.
738 Crippa, M., DeCarlo, P. F., Slowik, J. G., Mohr, C., Heringa, M. F., Chirico, R., Poulain, L., Freutel, F., Sciare, J.,
739 Cozic, J., Di Marco, C. F., Elsasser, M., Nicolas, J. B., Marchand, N., Abidi, E., Wiedensohler, A.,
740 Drewnick, F., Schneider, J., Borrmann, S., Nemitz, E., Zimmermann, R., Jaffrezo, J. L., Prevot, A. S. H.,
741 and Baltensperger, U.: Wintertime aerosol chemical composition and source apportionment of the organic
742 fraction in the metropolitan area of Paris, Atmos. Chem. Phys., 13, 961-981, https://doi.org/10.5194/acp-
743 13-961-2013, 2013.
744 Cross, E. S., Slowik, J. G., Davidovits, P., Allan, J. D., Worsnop, D. R., Jayne, J. T., Lewis, D. K., Canagaratna, M.,
745 and Onasch, T. B.: Laboratory and ambient particle density determinations using light scattering in
746 conjunction with aerosol mass spectrometry, Aerosol Sci. Technol., 41, 343-359,
747 https://doi.org/10.1080/02786820701199736, 2007.
748 Cross, E. S., Onasch, T. B., Canagaratna, M., Jayne, J. T., Kimmel, J., Yu, X. Y., Alexander, M. L., Worsnop, D. R.,
749 and Davidovits, P.: Single particle characterization using a light scattering module coupled to a time-of-
750 flight aerosol mass spectrometer, Atmos. Chem. Phys., 9, 7769-7793, https://doi.org/10.5194/acp-9-7769-
751 2009, 2009.
752 Davidson, C. I., Phalen, R. F., and Solomon, P. A.: Airborne particulate matter and human health: A review, Aerosol
753 Sci. Technol., 39, 737-749, https://doi.org/10.1080/02786820500191348, 2005.

DeCarlo, P. F., Slowik, J. G., Worsnop, D. R., Davidovits, P., and Jimenez, J. L.: Particle morphology and density characterization by combined mobility and aerodynamic diameter measurements. Part 1: Theory, Aerosol Sci. Technol., 38, 1185-1205, https://doi.org/10.1080/027868290903907, 2004.

Docherty, K. S., Aiken, A. C., Huffman, J. A., Ulbrich, I. M., DeCarlo, P. F., Sueper, D., Worsnop, D. R., Snyder, D. C., Peltier, R. E., Weber, R. J., Grover, B. D., Eatough, D. J., Williams, B. J., Goldstein, A. H., Ziemann, P. J., and Jimenez, J. L.: The 2005 Study of Organic Aerosols at Riverside (SOAR-1): instrumental intercomparisons and fine particle composition, Atmos. Chem. Phys., 11, 12387-12420, https://doi.org/10.5194/acp-11-12387-2011, 2011.

Docherty, K. S., Lewandowski, M., and Jimenez, J. L.: Effect of Vaporizer Temperature on Ambient Non-Refractory Submicron Aerosol Composition and Mass Spectra Measured by the Aerosol Mass Spectrometer, Aerosol Sci. Technol., 49, 485-494, https://doi.org/10.1080/02786826.2015.1042100, 2015.

Drewnick, F., Hings, S. S., DeCarlo, P., Jayne, J. T., Gonin, M., Fuhrer, K., Weimer, S., Jimenez, J. L., Demerjian, K. L., Borrmann, S., and Worsnop, D. R.: A new time-of-flight aerosol mass spectrometer (TOF-AMS) - Instrument description and first field deployment, Aerosol Sci. Technol., 39, 637-658, https://doi.org/10.1080/02786820500182040, 2005.

Elser, M., Huang, R. J., Wolf, R., Slowik, J. G., Wang, Q. Y., Canonaco, F., Li, G. H., Bozzetti, C., Daellenbach, K. R., Huang, Y., Zhang, R. J., Li, Z. Q., Cao, J. J., Baltensperger, U., El-Haddad, I., and Prevot, A. S. H.: New insights into PM2.5 chemical composition and sources in two major cities in China during extreme haze events using aerosol mass spectrometry, Atmos. Chem. Phys., 16, 3207-3225, https://doi.org/10.5194/acp-16-3207-2016, 2016.

Farmer, D. K., Matsunaga, A., Docherty, K. S., Surratt, J. D., Seinfeld, J. H., Ziemann, P. J., and Jimenez, J. L.: Response of an aerosol mass spectrometer to organonitrates and organosulfates and implications for atmospheric chemistry, Proceedings of the National Academy of Sciences of the United States of America, 107, 6670-6675, https://doi.org/10.1073/pnas.0912340107, 2010.

Fast, J., Aiken, A. C., Allan, J., Alexander, L., Campos, T., Canagaratna, M. R., Chapman, E., DeCarlo, P. F., de Foy, B., Gaffney, J., de Gouw, J., Doran, J. C., Emmons, L., Hodzic, A., Herndon, S. C., Huey, G., Jayne, J. T., Jimenez, J. L., Kleinman, L., Kuster, W., Marley, N., Russell, L., Ochoa, C., Onasch, T. B., Pekour, M., Song, C., Ulbrich, I. M., Warneke, C., Welsh-Bon, D., Wiedinmyer, C., Worsnop, D. R., Yu, X. Y., and Zaveri, R.: Evaluating simulated primary anthropogenic and biomass burning organic aerosols during MILAGRO: implications for assessing treatments of secondary organic aerosols, Atmos. Chem. Phys., 9, 6191-6215, 2009.

Gill, P. E., Murray, W., and Wright, M. H.: The Levenberg-Marquardt method, in: Practical optimization, Academic Press, London, 1981.

Griffith, S. M., Huang, X. H. H., Louie, P. K. K., and Yu, J. Z.: Characterizing the thermodynamic and chemical composition factors controlling PM2.5 nitrate: Insights gained from two years of online measurements in Hong Kong, Atmos. Environ., 122, 864-875, https://doi.org/10.1016/j.atmosenv.2015.02.009, 2015.

Guo, H., Wang, D. W., Cheung, K., Ling, Z. H., Chan, C. K., and Yao, X. H.: Observation of aerosol size distribution and new particle formation at a mountain site in subtropical Hong Kong, Atmos. Chem. Phys., 12, 9923-9939, https://doi.org/10.5194/acp-12-9923-2012, 2012.

Huang, X. F., He, L. Y., Hu, M., Canagaratna, M. R., Sun, Y., Zhang, Q., Zhu, T., Xue, L., Zeng, L. W., Liu, X. G., Zhang, Y. H., Jayne, J. T., Ng, N. L., and Worsnop, D. R.: Highly time-resolved chemical characterization of atmospheric submicron particles during 2008 Beijing Olympic Games using an Aerodyne High-Resolution Aerosol Mass Spectrometer, Atmos. Chem. Phys., 10, 8933-8945, https://doi.org/10.5194/acp-10-8933-2010, 2010.

Huang, X. F., He, L. Y., Hu, M., Canagaratna, M. R., Kroll, J. H., Ng, N. L., Zhang, Y. H., Lin, Y., Xue, L., Sun, T. L., Liu, X. G., Shao, M., Jayne, J. T., and Worsnop, D. R.: Characterization of submicron aerosols at a rural site in Pearl River Delta of China using an Aerodyne High-Resolution Aerosol Mass Spectrometer, Atmos. Chem. Phys., 11, 1865-1877, https://doi.org/10.5194/acp-11-1865-2011, 2011.

Huang, X. H. H., Bian, Q. J., Ng, W. M., Louie, P. K. K., and Yu, J. Z.: Characterization of PM2.5 Major Components and Source Investigation in Suburban Hong Kong: A One Year Monitoring Study, Aerosol Air Qual. Res., 14, 237-250, https://doi.org/10.4209/aaqr.2013.01.0020, 2014.

Huffman, J. A., Jayne, J. T., Drewnick, F., Aiken, A. C., Onasch, T., Worsnop, D. R., and Jimenez, J. L.: Design, modeling, optimization, and experimental tests of a particle beam width probe for the aerodyne aerosol mass spectrometer, Aerosol Sci. Technol., 39, 1143-1163, https://doi.org/10.1080/02786820500423782, 2005.

Jayne, J. T., Leard, D. C., Zhang, X. F., Davidovits, P., Smith, K. A., Kolb, C. E., and Worsnop, D. R.: Development of an aerosol mass spectrometer for size and composition analysis of submicron particles, Aerosol Sci. Technol., 33, 49-70, https://doi.org/10.1080/027868200410840, 2000.

Jimenez, J. L., Jayne, J. T., Shi, Q., Kolb, C. E., Worsnop, D. R., Yourshaw, I., Seinfeld, J. H., Flagan, R. C., Zhang, X. F., Smith, K. A., Morris, J. W., and Davidovits, P.: Ambient aerosol sampling using the Aerodyne Aerosol Mass Spectrometer, J. Geophys. Res. Atmos., 108, 8425, https://doi.org/10.1029/2001jd001213, 2003.

John, W.: Size Distribution Characteristics of Aerosols, in: Aerosol Measurement, John Wiley & Sons, Inc., 41-54, 2011.

Kerminen, V. M., Paramonov, M., Anttila, T., Riipinen, I., Fountoukis, C., Korhonen, H., Asmi, E., Laakso, L., Lihavainen, H., Swietlicki, E., Svenningsson, B., Asmi, A., Pandis, S. N., Kulmala, M., and Petaja, T.: Cloud condensation nuclei production associated with atmospheric nucleation: a synthesis based on existing literature and new results, Atmos. Chem. Phys., 12, 12037-12059, https://doi.org/10.5194/acp-12-12037-2012, 2012.

Knote, C., Brunner, D., Vogel, H., Allan, J., Asmi, A., Aijala, M., Carbone, S., van der Gon, H. D., Jimenez, J. L., Kiendler-Scharr, A., Mohr, C., Poulain, L., Prevot, A. S. H., Swietlicki, E., and Vogel, B.: Towards an online-coupled chemistry-climate model: evaluation of trace gases and aerosols in COSMO-ART, Geosci. Model Dev., 4, 1077-1102, https://doi.org/10.5194/gmd-4-1077-2011, 2011.

Köhler, H.: The nucleus in and the growth of hygroscopic droplets, Trans. Faraday Soc., 32, 1152-1161, https://doi.org/10.1039/tf9363201152, 1936.

Lee, B. P., Li, Y. J., Yu, J. Z., Louie, P. K. K., and Chan, C. K.: Physical and chemical characterization of ambient aerosol by HR-ToF-AMS at a suburban site in Hong Kong during springtime 2011, J. Geophys. Res. Atmos., 118, 8625-8639, https://doi.org/10.1002/jgrd.50658, 2013.

Lee, B. P., Li, Y. J., Yu, J. Z., Louie, P. K. K., and Chan, C. K.: Characteristics of submicron particulate matter at the urban roadside in downtown Hong Kong-Overview of 4 months of continuous high-resolution aerosol mass spectrometer measurements, J. Geophys. Res. Atmos.,, 120, 7040-7058, https://doi.org/10.1002/2015jd023311, 2015.

Li, Y. J., Lee, B. Y. L., Yu, J. Z., Ng, N. L., and Chan, C. K.: Evaluating the degree of oxygenation of organic aerosol during foggy and hazy days in Hong Kong using high-resolution time-of-flight aerosol mass spectrometry (HR-ToF-AMS), Atmos. Chem. Phys., 13, 8739-8753, https://doi.org/10.5194/acp-13-8739-2013, 2013.

Li, Y. J., Lee, B. P., Su, L., Fung, J. C. H., and Chan, C. K.: Seasonal characteristics of fine particulate matter (PM) based on high-resolution time-of-flight aerosol mass spectrometric (HR-ToF-AMS) measurements at the HKUST Supersite in Hong Kong, Atmos. Chem. Phys., 15, 37-53, https://doi.org/10.5194/acp-15-37-2015, 2015.

Liu, P. S. K., Deng, R., Smith, K. A., Williams, L. R., Jayne, J. T., Canagaratna, M. R., Moore, K., Onasch, T. B., Worsnop, D. R., and Deshler, T.: Transmission efficiency of an aerodynamic focusing lens system: Comparison of model calculations and laboratory measurements for the Aerodyne Aerosol Mass Spectrometer, Aerosol Sci. Technol., 41, 721-733, https://doi.org/10.1080/02786820701422278, 2007.

Man, H., Zhu, Y., Ji, F., Yao, X., Lau, N. T., Li, Y., Lee, B. P., and Chan, C. K.: Comparison of daytime and nighttime new particle growth at the HKUST supersite in Hong Kong, Environ. Sci. Technol., 49, 7170-7178, https://doi.org/10.1021/acs.est.5b02143, 2015.

Meng, J. W., Yeung, M. C., Li, Y. J., Lee, B. Y. L., and Chan, C. K.: Size-resolved cloud condensation nuclei (CCN) activity and closure analysis at the HKUST Supersite in Hong Kong, Atmos. Chem. Phys., 14, 10267-10282, https://doi.org/10.5194/acp-14-10267-2014, 2014.

Middlebrook, A. M., Bahreini, R., Jimenez, J. L., and Canagaratna, M. R.: Evaluation of Composition-Dependent Collection Efficiencies for the Aerodyne Aerosol Mass Spectrometer using Field Data, Aerosol Sci. Technol., 46, 258-271, https://doi.org/10.1080/02786826.2011.620041, 2012.

Mohr, C., DeCarlo, P. F., Heringa, M. F., Chirico, R., Slowik, J. G., Richter, R., Reche, C., Alastuey, A., Querol, X., Seco, R., Penuelas, J., Jimenez, J. L., Crippa, M., Zimmermann, R., Baltensperger, U., and Prevot, A. S. H.: Identification and quantification of organic aerosol from cooking and other sources in Barcelona using aerosol mass spectrometer data, Atmos. Chem. Phys., 12, 1649-1665, https://doi.org/10.5194/acp-12-1649-2012, 2012.

Quinn, P. K., Bates, T. S., Coffman, D., Onasch, T. B., Worsnop, D., Baynard, T., de Gouw, J. A., Goldan, P. D., Kuster, W. C., Williams, E., Roberts, J. M., Lerner, B., Stohl, A., Pettersson, A., and Lovejoy, E. R.:

Impacts of sources and aging on submicrometer aerosol properties in the marine boundary layer across the Gulf of Maine, J. Geophys. Res. Atmos., 111, D23S36, https://doi.org/10.1029/2006jd007582, 2006.

Rupakheti, M., Leaitch, W. R., Lohmann, U., Hayden, K., Brickell, P., Lu, G., Li, S. M., Toom-Sauntry, D., Bottenheim, J. W., Brook, J. R., Vet, R., Jayne, J. T., and Worsnop, D. R.: An intensive study of the size and composition of submicron atmospheric aerosols at a rural site in Ontario, Canada, Aerosol Sci. Technol., 39, 722-736, https://doi.org/10.1080/02786820500182420, 2005.

Saarikoski, S., Carbone, S., Decesari, S., Giulianelli, L., Angelini, F., Canagaratna, M., Ng, N. L., Trimborn, A., Facchini, M. C., Fuzzi, S., Hillamo, R., and Worsnop, D.: Chemical characterization of springtime submicrometer aerosol in Po Valley, Italy, Atmos. Chem. Phys., 12, 8401-8421, https://doi.org/10.5194/acp-12-8401-2012, 2012.

Salcedo, D., Onasch, T. B., Dzepina, K., Canagaratna, M. R., Zhang, Q., Huffman, J. A., DeCarlo, P. F., Jayne, J. T., Mortimer, P., Worsnop, D. R., Kolb, C. E., Johnson, K. S., Zuberi, B., Marr, L. C., Volkamer, R., Molina, L. T., Molina, M. J., Cardenas, B., Bernabe, R. M., Marquez, C., Gaffney, J. S., Marley, N. A., Laskin, A., Shutthanandan, V., Xie, Y., Brune, W., Lesher, R., Shirley, T., and Jimenez, J. L.: Characterization of ambient aerosols in Mexico City during the MCMA-2003 campaign with Aerosol Mass Spectrometry: results from the CENICA Supersite, Atmos. Chem. Phys., 6, 925-946, 2006.

Schwartz, S. E.: The Whitehouse effect - Shortwave radiative forcing of climate by anthropogenic aerosols: An overview, J. Aerosol Sci, 27, 359-382, https://doi.org/10.1016/0021-8502(95)00533-1, 1996.

Seinfeld, J. H., and Pandis, S. N.: Atmospheric Chemistry and Physics - From Air Pollution to Climate Change, 2 ed., John Wiley & Sons, 2006.

Setyan, A., Zhang, Q., Merkel, M., Knighton, W. B., Sun, Y., Song, C., Shilling, J. E., Onasch, T. B., Herndon, S. C., Worsnop, D. R., Fast, J. D., Zaveri, R. A., Berg, L. K., Wiedensohler, A., Flowers, B. A., Dubey, M. K., and Subramanian, R.: Characterization of submicron particles influenced by mixed biogenic and anthropogenic emissions using high-resolution aerosol mass spectrometry: results from CARES, Atmos. Chem. Phys., 12, 8131-8156, https://doi.org/10.5194/acp-12-8131-2012, 2012.

Slowik, J. G., Stainken, K., Davidovits, P., Williams, L. R., Jayne, J. T., Kolb, C. E., Worsnop, D. R., Rudich, Y., DeCarlo, P. F., and Jimenez, J. L.: Particle morphology and density characterization by combined mobility and aerodynamic diameter measurements. Part 2: Application to combustion-generated soot aerosols as a function of fuel equivalence ratio, Aerosol Sci. Technol., 38, 1206-1222, https://doi.org/10.1080/027868290903916, 2004.

Sun, C., Lee, B. P., Huang, D., Li, Y. J., Schurman, M. I., Louie, P. K. K., Luk, C., and Chan, C. K.: Continuous measurements at the urban roadside in an Asian megacity by Aerosol Chemical Speciation Monitor (ACSM): particulate matter characteristics during fall and winter seasons in Hong Kong, Atmos. Chem. Phys., 16, 1713-1728, https://doi.org/10.5194/acp-16-1713-2016, 2016.

Sun, Y., Zhang, Q., Macdonald, A. M., Hayden, K., Li, S. M., Liggio, J., Liu, P. S. K., Anlauf, K. G., Leaitch, W. R., Steffen, A., Cubison, M., Worsnop, D. R., van Donkelaar, A., and Martin, R. V.: Size-resolved aerosol

chemistry on Whistler Mountain, Canada with a high-resolution aerosol mass spectrometer during INTEX-B, Atmos. Chem. Phys., 9, 3095-3111, https://doi.org/10.5194/acp-9-3095-2009, 2009.

Sun, Y. L., Zhang, Q., Schwab, J. J., Demerjian, K. L., Chen, W. N., Bae, M. S., Hung, H. M., Hogrefe, O., Frank, B., Rattigan, O. V., and Lin, Y. C.: Characterization of the sources and processes of organic and inorganic aerosols in New York city with a high-resolution time-of-flight aerosol mass apectrometer, Atmos. Chem. Phys., 11, 1581-1602, https://doi.org/10.5194/acp-11-1581-2011, 2011.

Takegawa, N., Miyakawa, T., Watanabe, M., Kondo, Y., Miyazaki, Y., Han, S., Zhao, Y., van Pinxteren, D., Bruggemann, E., Gnauk, T., Herrmann, H., Xiao, R., Deng, Z., Hu, M., Zhu, T., and Zhang, Y.: Performance of an Aerodyne Aerosol Mass Spectrometer (AMS) during Intensive Campaigns in China in the Summer of 2006, Aerosol Sci. Technol., 43, 189-204, https://doi.org/10.1080/02786820802582251, 2009.

Ulbrich, I. M., Canagaratna, M. R., Cubison, M. J., Zhang, Q., Ng, N. L., Aiken, A. C., and Jimenez, J. L.: Three-dimensional factorization of size-resolved organic aerosol mass spectra from Mexico City, Atmos. Meas. Tech., 5, 195-224, https://doi.org/10.5194/amt-5-195-2012, 2012.

Westervelt, D. M., Pierce, J. R., Riipinen, I., Trivitayanurak, W., Hamed, A., Kulmala, M., Laaksonen, A., Decesari, S., and Adams, P. J.: Formation and growth of nucleated particles into cloud condensation nuclei: model-measurement comparison, Atmos. Chem. Phys., 13, 7645-7663, https://doi.org/10.5194/acp-13-7645-2013, 2013.

Williams, L. R., Gonzalez, L. A., Peck, J., Trimborn, D., McInnis, J., Farrar, M. R., Moore, K. D., Jayne, J. T., Robinson, W. A., Lewis, D. K., Onasch, T. B., Canagaratna, M. R., Trimborn, A., Timko, M. T., Magoon, G., Deng, R., Tang, D., Blanco, E. D. L. R., Prevot, A. S. H., Smith, K. A., and Worsnop, D. R.: Characterization of an aerodynamic lens for transmitting particles greater than 1 micrometer in diameter into the Aerodyne aerosol mass spectrometer, Atmos. Meas. Tech., 6, 3271-3280, https://doi.org/10.5194/amt-6-3271-2013, 2013.

Yao, X., Ling, T. Y., Fang, M., and Chan, C. K.: Size dependence of in situ pH in submicron atmospheric particles in Hong Kong, Atmos. Environ., 41, 382-393, https://doi.org/10.1016/j.atmosenv.2006.07.037, 2007a.

Yao, X. H., Lau, N. T., Chan, C. K., and Fang, M.: Size distributions and condensation growth of submicron particles in on-road vehicle plumes in Hong Kong, Atmos. Environ., 41, 3328-3338, https://doi.org/10.1016/j.atmosenv.2006.12.044, 2007b.

Yuan, Z. B., Yadav, V., Turner, J. R., Louie, P. K. K., and Lau, A. K. H.: Long-term trends of ambient particulate matter emission source contributions and the accountability of control strategies in Hong Kong over 1998-2008, Atmos. Environ., 76, 21-31, https://doi.org/10.1016/j.atmosenv.2012.09.026, 2013.

Zhang, J. K., Sun, Y., Liu, Z. R., Ji, D. S., Hu, B., Liu, Q., and Wang, Y. S.: Characterization of submicron aerosols during a month of serious pollution in Beijing, 2013, Atmos. Chem. Phys., 14, 2887-2903, https://doi.org/10.5194/acp-14-2887-2014, 2014.

Zhang, Q., Stanier, C. O., Canagaratna, M. R., Jayne, J. T., Worsnop, D. R., Pandis, S. N., and Jimenez, J. L.: Insights into the chemistry of new particle formation and growth events in Pittsburgh based on aerosol mass spectrometry, Environ. Sci. Technol., 38, 4797-4809, https://doi.org/10.1021/es035417u, 2004.

Zhang, Q., Canagaratna, M. R., Jayne, J. T., Worsnop, D. R., and Jimenez, J. L.: Time- and size-resolved chemical composition of submicron particles in Pittsburgh: Implications for aerosol sources and processes, J. Geophys. Res. Atmos., 110, https://doi.org/10.1029/2004jd004649, 2005.

Zheng, M., Kester, D. R., Wang, F., Shi, X. M., and Guo, Z. G.: Size distribution of organic and inorganic species in Hong Kong aerosols during the wet and dry seasons, J. Geophys. Res. Atmos., 113, D16303, https://doi.org/10.1029/2007jd009494, 2008.

Zhuang, H., Chan, C. K., Fang, M., and Wexler, A. S.: Size distributions of particulate sulfate, nitrate, and ammonium at a coastal site in Hong Kong, Atmos. Environ., 33, 843-853, https://doi.org/10.1016/S1352-2310(98)00305-7, 1999.